Nonlinear Processes
in Geophysics

Open Access

Nonlinear dynamics approach to the predictability of the Cane–Zebiak coupled ocean–atmosphere model

L. Siqueira and B. Kirtman

Rosenstiel School of Marine and Atmospheric Science, University of Miami, Miami, USA

Correspondence to: L. Siqueira (lsiqueira@rsmas.miami.edu)

Abstract. The predictability of the Cane–Zebiak coupled ocean–atmosphere model is investigated using nonlinear dynamics analysis. Newer theoretical concepts are applied to the coupled model in order to help quantify maximal prediction horizons for finite amplitude perturbations on different scales. Predictability analysis based on the maximum Lyapunov exponent considers infinitesimal perturbations, which are associated with errors in the smallest fastest-evolving scales of motion. However, these errors become irrelevant for the predictability of larger scale motions. In this study we employed finite-size Lyapunov exponent analysis to assess the predictability of the Cane–Zebiak coupled ocean–atmosphere model as a function of scale. We demonstrate the existence of fast and slow timescales, as noted in earlier studies, and the expected enhanced predictability of the anomalies on large scales. The final results and conclusions clarify the applicability of these new methods to seasonal forecasting problems.

1 Introduction

The fundamental question regarding the predictability limits of the coupled ocean–atmosphere system has not been well established yet, although recent coupled models are able to forecast phenomena like El Niño–Southern Oscillation (ENSO) up to about one year in advance (Kirtman and Min, 2009). The atmospheric predictability has been extensively investigated in the past, and classical predictability studies (Lorenz, 1965, 1969; Charney et al., 1966; Smagorinsky, 1969; Shukla, 1985) have established that the instantaneous state of the atmosphere cannot be predicted beyond a few weeks. However, only a few studies have examined the predictability of the coupled ocean–atmosphere system. Un-

certainties in the atmospheric state are passed to the ocean through coupling processes. The predictability of the coupled system depends critically on how uncertainties in the atmospheric state reach nonlinear equilibrium, and how this relatively high-frequency noise interacts with the low-frequency evolution of the ocean model (Goswami et al., 1997). Within the atmosphere, a similar reasoning for the predictability dependence on 2-D turbulence interacting with 3-D turbulence also applies. The tropical Pacific coupled ocean–atmosphere system with its primary oscillatory instability, i.e., ENSO, is an interesting example of a coupled fast–slow system of crucial importance for seasonal forecasting, and is the focus of this study.

In the early 90s, Goswami and Shukla (1991) and Blumenthal (1991), following different procedures but using the same model, showed that the growth of errors in the Cane–Zebiak coupled model (Zebiak and Cane, 1987) is governed by two different timescales. However, none of these studies involving the predictability of the coupled ocean–atmosphere system made use of methods from nonlinear dynamics analysis available today. Newer theoretical concepts are available to reveal the detailed structure of the observed or modeled variability in a condensed way, providing additional conceptual insight as well as quantifying maximal prediction horizons that have useful applicability to seasonal forecasting problems like ENSO.

Classical predictability analysis based on the maximum Lyapunov exponent (MLE) considers infinitesimal perturbations (Rosenstein et al., 1993; Kantz, 1994), which are associated with errors in the smallest fastest-evolving scales of motion as in Eq. (1). However, the Lyapunov exponent and its association with prediction horizons (Boffetta et al., 1998a) are of very limited use in multiple timescale systems like geophysical flows, and predictions can actually be made

far beyond the characteristic Lyapunov timescale. The MLE can be defined as

$$\lambda = \lim_{t \to \infty} \lim_{\delta_x^0 \to 0} \frac{1}{t} \ln \frac{|\delta x(t)|}{|\delta_x^0|}, \qquad (1)$$

where $\delta_x^0 = \delta x(0)$ represents an infinitesimal initial uncertainty in the model state. Because the initial conditions can be measured only with a finite uncertainty $\delta x(0)$, we can forecast the future state of the system with a given error tolerance level Δ only to a maximum time T_p (prediction horizon)

$$T_p = \frac{1}{\lambda} \ln \frac{\Delta}{\delta x(0)}. \qquad (2)$$

Equation (2) gives the shortest prediction horizon, which is associated with the smallest, low energy-containing scales that, as soon as their error reaches nonlinear saturation, do not play a role in the error growth. Larger errors, which typically occur at larger scales, will grow at a different rate. This is usually due to the small-scale instabilities growing faster but becoming nonlinearly saturated at a much smaller level than large-scale instabilities. In general, large errors will grow with the characteristic timescale of the largest slow-evolving high-energy containing scales. It is worth noting at this point that the largest energy-containing scales are associated with instabilities that obtain energy from the mean flow and also from each other. Thus these are the energy production instabilities that contain most of the energy, but are not the same as the largest scales in space and time. Therefore, the effect of the smallest fast-evolving scales (considered by the MLE analysis) becomes irrelevant for the predictability of larger scale motions.

In order to overcome this problem associated with the infinitesimally small amplitude perturbations, Aurell et al. (1997) have generalized the Lyapunov exponent concept to non-infinitesimal finite amplitude perturbations. The finite-size Lyapunov exponent (FSLE) is particularly useful when there exist characteristic scales; this allows the computation of the average exponential error growth at a given scale, say, δ. This generalization has the advantage that both the nonlinear dynamical evolution of these perturbations as well as the predictability of multiple timescale systems can be treated appropriately (Boffetta et al., 1998a). The finite-size Lyapunov exponent $\lambda(\delta)$ is based on the concept of error growing time $\tau_q(\delta)$ (error q-pling time), which is the smallest time it takes for a perturbation of initial size δ to grow by a factor q.

To practically compute the FSLE, we assume that a system has been evolved for long enough that the transient dynamics has lapsed, e.g., for dissipative systems the motion has settled onto the attractor. Then we consider at $t = 0$ a "reference" trajectory $x(0)$ supposed to be on the attractor, and generate a "perturbed" trajectory $x'(0) = x(0) + \delta x(0)$. We need the perturbation to be initially very small (essentially infinitesimal) in some chosen norm $\delta(t = 0) = \parallel \delta x(t = 0) \parallel = \delta_{\min} \ll 1$. Typically, in numerical experiments

with "toy models" $\delta_{\min} = \mathcal{O}(10^{-6} - 10^{-8})$, but for intermediate complexity models like the Cane–Zebiak coupled model and in a state-of-the-art coupled general circulation model (CGCM), $\delta_{\min}$ is limited by the precision of the finite data set that leads to a minimum length scale below which the attractor structure cannot be resolved (later shown in Sect. 4). Then, in order to study the perturbation growth through different scales, we can define a series of thresholds, $\delta_n = q^n \delta_0$, and to measure the time $\tau_q(\delta)$ that a perturbation with size δ_n takes to grow up to δ_{n+1}, where $n = 0, \ldots, N_s$ represents an increasing scale and N_s is the scale at which the error saturates. The ratio q should not be taken too large in order to avoid interference due to the growth through different scales before reaching the next threshold. On the other hand, the rate q cannot be too close to one; typically a sensible threshold rate is $q = 2$ (which we take throughout this work) or $q = \sqrt{2}$. The choice of $q = 2$ leads to the "doubling time" τ_2, while $q = e$ yields the so-called "e-folding time". Both doubling time and e-folding time are frequently used in the literature to characterize error growth; thus, we pick the doubling time as a convenient number for comparison with previous work on CZ predictability (Goswami and Shukla, 1991; Blumenthal, 1991; Goswami et al., 1997). The time $\tau_q(\delta)$ is obtained by integrating two trajectories of the system that start at an initial distance $\delta_{\min}$ and this process is illustrated in Fig. 1.

The algorithm schematized in Fig. 1 proceeds as follows. After time t_0, the perturbation has grown from $\delta_{\min}$ up to δ_n, ensuring that the perturbed trajectory relaxes on the attractor and aligns along the maximally expanding direction. Then, we measure the time $\tau_1(\delta_n)$, the error needed to grow up to δ_{n+1}, i.e., the first time such that $\delta(t_0) = \parallel \delta x(t_0) \parallel = \delta_n$ and $\delta(t_0 + \tau_1(\delta_n)) = \delta_{n+1}$. The perturbation is thus rescaled to δ_n, along the direction $x' - x$ (see Fig. 1). The procedure is repeated $\mathcal{N}_d$ times for each threshold, obtaining the set of the "doubling" times (strictly speaking the name applies for $q = 2$ only) $\{\tau_i(\delta_n)\}$ for $i = 1, \ldots, \mathcal{N}_d$ error-doubling experiments. Note that $\tau(\delta_n)$ also depends on q. The doubling rate is defined as

$$\gamma_i(\delta_n) = \frac{1}{\tau_i(\delta_n)} \ln q. \qquad (3)$$

The error growing time is a fluctuating quantity and one has to take the average along the trajectory as in Eq. (1), therefore the FSLE $\lambda(\delta)$ is computed by taking the average over the natural measure along the trajectory (invariant measure of the dynamics), which is approximated by the ensemble average $\langle \cdot \rangle_{\mathrm{ens}}$ over many realizations.

$$\lambda(\delta_n) = \langle \gamma(\delta_n) \rangle_t = \frac{1}{T} \int_0^T dt \, \gamma = \frac{\sum_i \gamma_i \tau_i}{\sum_i \tau_i} \qquad (4)$$
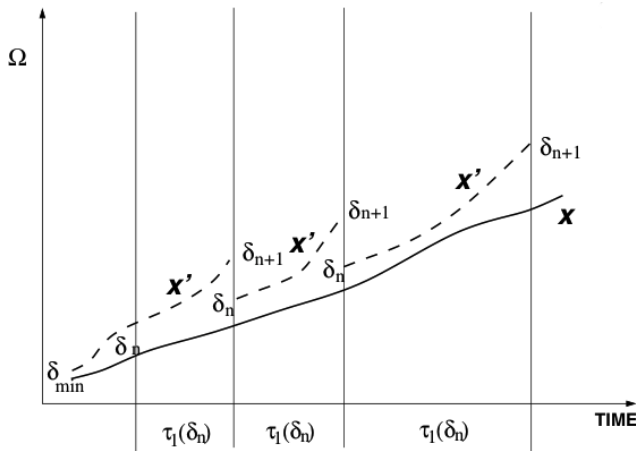
Fig. 1. Finite-size Lyapunov exponent algorithm schematized after Boffetta et al. (1998a).

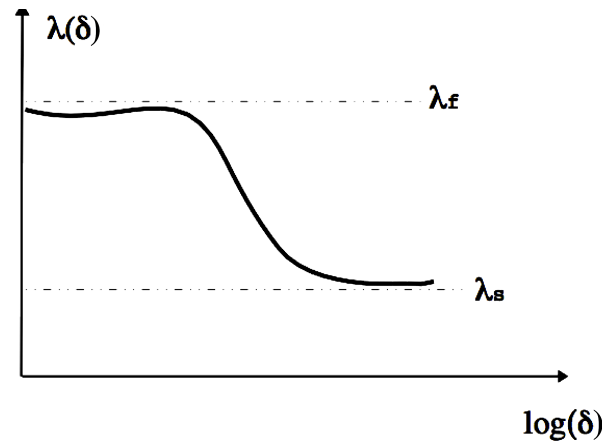**Fig. 2.** Finite-size Lyapunov exponent of two coupled (slow–fast) Lorenz models computed from the slow variables. The two horizontal lines represent the uncoupled Lyapunov exponents. Figure schematized after Boffetta et al. (1998a).

using Eq. (3) yields

$$\lambda(\delta_n) = \frac{1}{\langle \tau(\delta_n) \rangle_d} \ln q, \tag{5}$$

where $\langle \tau(\delta) \rangle_d = \sum_i \tau_i / \mathcal{N}_d$ is the average over the doubling experiments and the total duration of the trajectory is $T = \sum_i \tau_i$. When δ_n is infinitesimal, $\lambda(\delta_n)$ recovers the MLE, in Eq. (1), and we have $\lim_{\delta \to 0} \lambda(\delta_n) = \lambda_1$. We must underline two things: (i) unlike the standard LE, when δ is finite $\lambda(\delta)$ depends on the chosen norm and this dependence is a manifestation of the fact that in the nonlinear regime the predictability time depends on the chosen observable; (ii) since the FSLE is based on "q-pling" times, it cannot detect negative LEs.

Boffetta et al. (1998a) illustrated this new concept by studying two coupled sets of nonlinear Lorenz (1963) aligns, one characterized by a slow and the other one characterized by a fast timescale. They showed that the FSLE is indeed an adequate quantity to describe the predictability of systems with multiple timescales. The FSLE is expected to converge to the leading Lyapunov exponent λ_f of the fast decoupled system for small scales, whereas for large scales it asymptotically approaches the Lyapunov exponent λ_s of the slow decoupled system (Fig. 2).

It is worth noting that Fig. 2, schematized after Boffetta et al. (1998a), does not illustrate the fact that if the phase space is bounded, then $\lambda(\delta)$ goes to zero for sufficiently large δ, simply because the distance between two trajectories cannot grow without bound on a bounded phase space. This is later shown for the CZ model in Figs. 7 and 8 in Sect. 4 (Results).

One interesting fact is that the MLE defined in Eq. (1) does not depend on the initial state, but for the FSLE one has to take an average over initial states in Eq. (5). Since the FSLE depends on the initial state, one can consider the application of the FSLE for a particular season (ENSO spring predictability barrier) or regime of the system as in Mitchell and Gottwald (2012). In order to consider the FSLE seasonal or regime dependence, the algorithm can be modified to avoid the rescaling at finite δ_n as follows. The thresholds $\{\delta_n\}$ and the initial perturbation ($\delta_{min} \ll \delta_0$) are chosen as before, but now the perturbation growth is followed from δ_0 to δ_{N_s} without rescaling back the perturbation once the threshold is reached. In practice, after the system reaches the first threshold δ_0, we measure the time $\tau_1(\delta_0)$ to reach δ_1, then following the same perturbed trajectory we measure the time $\tau_1(\delta_1)$ to reach δ_2, and so forth up to δ_{N_s}: we thus record the time $\tau(\delta_n)$ for going from δ_n to δ_{n+1} for each value of n. One important difference in the modified algorithm is that the evolution of the error from the initial value δ_{min} to the largest threshold δ_{N_s} carries out a single error-doubling experiment. Therefore, it relies on the realization of an ensemble of simulations in order to take the average over many realizations with different initial conditions for a particular season or regime of the system.

In order to quantify the typical predictability time for a trajectory with initial uncertainty δ, we introduce the average error growing time for a trajectory with initial uncertainty δ and a given tolerance Δ as

$$T_p(\Delta, \delta) = \int_\delta^\Delta \frac{d \ln \delta'}{\lambda(\delta')}, \tag{6}$$

which reduce to Eq. (2) in the case of constant λ. Furthermore, from the considerations mentioned above, one expects that $\lambda(\delta)$ is a decreasing function of δ and thus Eq. (6) gives longer predictability time than Eq. (2).

In the case studied by Boffetta et al. (1998a) the prediction horizon T_p of the slow component of the coupled fast-slow Lorenz (1963) system becomes orders of magnitude larger
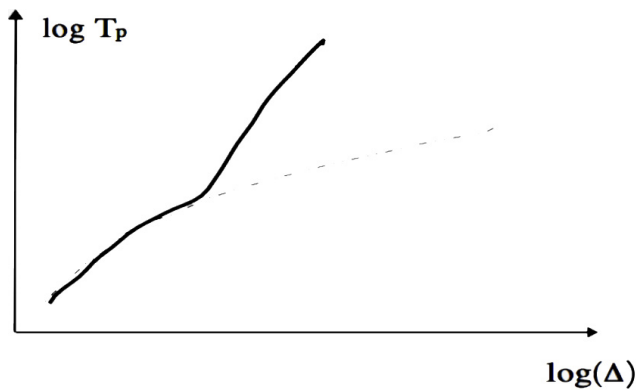
Fig. 3. Average error growing time T_{p} for the slow component of the two coupled Lorenz models as a function of error tolerance Δ. The dashed line represents the classical Lyapunov estimate. Figure schematized after Boffetta et al. (1998a).

Fig. 4. Sea surface temperature anomalies in the NINO3 ($5°$ S– $5°$ N; 150–$90°$ W) region from a $50\,000$ yr run of the CZ model (monthly means from the first thousand years).

than the one based on the classical Lyapunov estimate, when large error tolerances are allowed, which is shown in Fig. 3.

The interest in error growth rates and their influence on the predictability has also promoted the development of breeding vectors, which are optimal finite-size perturbations that represent the directions of growing analysis errors to produce optimal perturbations for ensemble forecasting (Toth and Kalnay, 1993, 1997; Vikhliaev et al., 2007). The average growth rate of the breeding vectors, which are also scale dependent, is closely related to the FSLE (Boffetta et al., 2002; Peña and Kalnay, 2004). An interesting property of the FSLE methodology as presented here is that it also applies to systems that are forced or partly forced by noise.

2 The model

In this study we used the standard version of the Cane– Zebiak (CZ) model that has been used in a large number of studies related to ENSO (Zebiak and Cane, 1987; Goswami and Shukla, 1991, 1993; Blumenthal, 1991). This is an anomaly coupled model, i.e., the governing aligns represent oceanic and atmospheric perturbations about the mean climatological state, with monthly climatology prescribed from observation. The nonlinearity enters through the thermodynamic energy align for the ocean and the model does not contain the high-frequency internal variability in the atmosphere since it considers a steady-state atmosphere. It is worth noting that this is in contrast with the real coupled ocean–atmosphere system discussed in the Introduction, since in the CZ model the nonlinearities and high-frequency variability do not enter through the atmosphere.

In this paper, we performed a $50\,000$ yr-long run of the CZ model to quantify its predictability. The coupled model run is able to simulate important aspects of interannual variations in the tropical Pacific reasonably realistically, contain nonlinearity, and shows a timescale similar to the observed
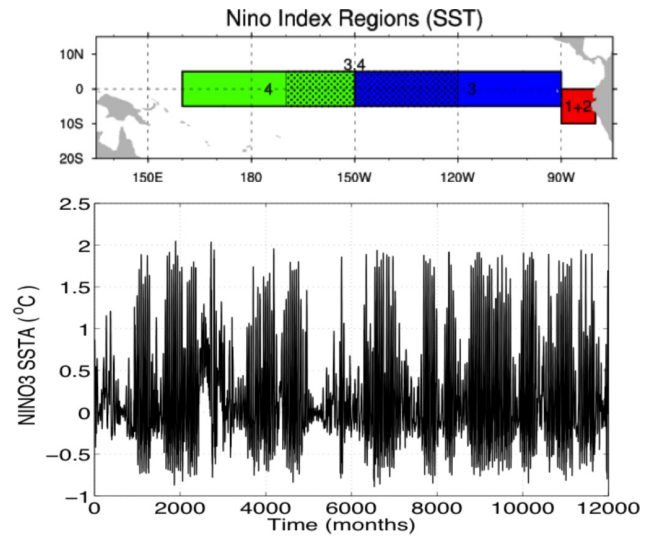
system. The model is able to simulate the characteristic large-scale spatial (not shown) and temporal structure of ENSO (see Zebiak and Cane, 1987). The evolution of mean monthly sea surface temperature anomalies in the NINO3 region of the eastern tropical Pacific ($5°$ S–$5°$ N; 150–$90°$ W) is shown in Fig. 4. The choice of this region to represent the system's evolution is based on the fact that this is the region of the tropical Pacific that has the largest variability in sea surface temperature on interannual timescales and is highly correlated with the dominant mode of variability, i.e., the first EOF of the system (not shown). The evolution is clearly irregular, with decades of little activity and decades of irregular cycles of warm and cold phases with an average period of 3–4 yr. The chaotic dynamics of the model is due to the fact that the SST align and the atmospheric heating are nonlinear.

3 Methodology

Previous predictability experiments involving the CZ model were conducted introducing small perturbations distributed randomly in space in Goswami and Shukla (1991), which actually introduces perturbations in all scales of motion, or by representing the fields in terms of its EOFs, and then studying the evolution of uncertainties that have the spatial structure of one of them (Blumenthal, 1991).

The methodology employed here differs from the previous studies, since it is based on newer theoretical concepts from nonlinear dynamics analysis and follows the following steps. First, we reconstruct the system dynamics in phase space using the Takens embedding theorem (Takens, 1981; Sauer et al., 1991) and then apply the finite-size Lyapunov exponent algorithm in order to infer the CZ model predictability.

A similar procedure could be done using an EOF reduction to reconstruct the system's phase space, since the NINO3 index is highly correlated with the first EOF.

4   Results

The choice of optimal embedding is crucial for reconstructing the system dynamics in phase space as well as for the application of the FSLE algorithm in order to infer the CZ model predictability. Given the NINO3 index, which is a scalar series, a suitable delay time and an embedding dimension were chosen following the methods of mutual information and correlation dimension, respectively (Kantz and Schreiber, 2004).

We determined a suitable delay time based on the autocorrelation function and mutual information, since one criterion may be superior for one dynamical system and poor for another. The optimal delay is estimated by the first minimum of mutual information (when it has a minimum) or when the autocorrelation drops below $1/e$ or has a point of inflection (Albano et al., 1988; Fraser and Swinney, 1986). Figure 5 shows the autocorrelation and mutual information as a function of the time lags for the CZ model, suggesting a delay time of 9–10 months. Note that the autocorrelation for $\tau = 50$ months is well above the $1/e$ threshold. This indicates that the Cane–Zebiak model is predictable at least 50 months ahead, much longer than the predictability of real ENSO by current systems.

We also need to estimate the dimensionality of the system to perform the phase space reconstruction. The curves for the correlation dimension (Grassberger and Procaccia, 1983) of the CZ model NINO3 index in Fig. 6 show a scaling range where all curves saturate (plateau) slightly below 4, giving the estimated dimensionality of the signal. The low value of saturation of the slopes reveals that the underlying dynamics of the CZ model correspond to a low-dimensional deterministic process. According to the embedding theory, the dynamical degrees of freedom cannot be higher than $2D+1 = 9$ and lower than $D_{\mathrm{int}} \approx 4$ where D_{int} is the first integer value after the saturation value. The size of the 50 000 yr simulation, with monthly outputs of the CZ model, implies that the highest dimension attractor that can be discerned using this time series is between 9 and 10 dimensions according to Tsonis (1992).

Our result is in agreement with the dimensionality estimate of 3.5 for the CZ model obtained by Tziperman et al. (1994). It is worth noting that the ocean component of this model is essentially made up of two prognostic aligns, one for the mixed layer thermodynamics align for SST, a thermocline depth align for upper ocean dynamics, along with SST-gradient-wind relation, and the wind-equatorial upwelling relation. This implies roughly 4 degrees of freedom and therefore this data set is expected to be low dimensional.
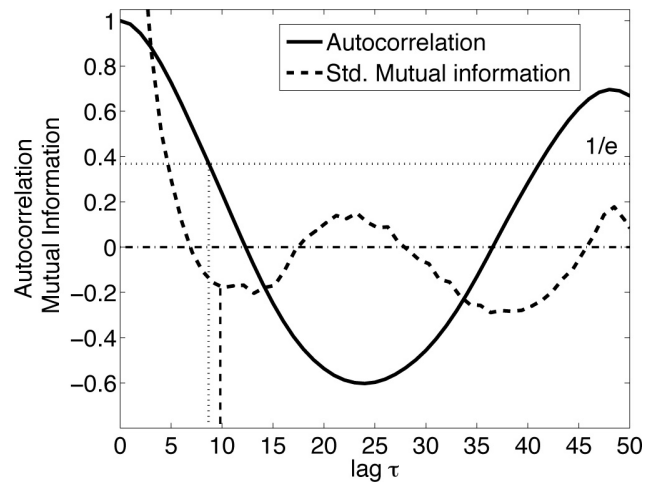

Fig. 5. Autocorrelation function of the NINO3 index (solid line) and mutual information (dashed line) at different time lags for the CZ model.
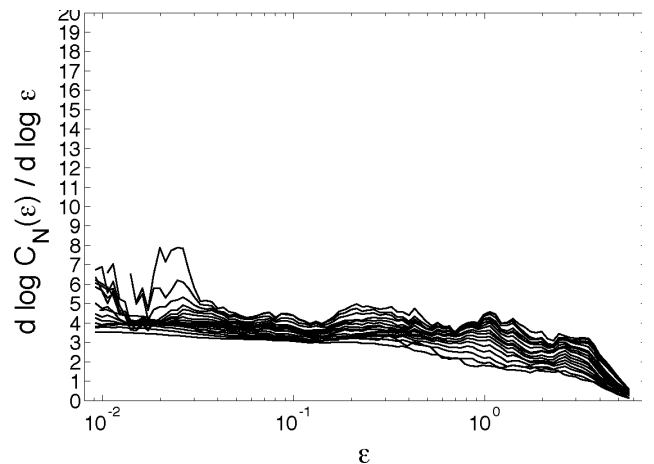
Fig. 6. The correlation dimension (local slopes of the correlation integral) of the NINO3 index of the CZ model. Embedding is done with a delay of 10 months. The different curves represent $m = 4, \ldots, 20$ dimensions (from bottom to top).

We reconstruct the CZ model phase space using the Takens embedding theorem (Takens, 1981; Sauer et al., 1991) applied to the NINO3 index time series. The dynamics in phase space appears as a chaotic attractor (fractal) where the interannual oscillations clearly display low-order deterministic chaos (Fig. 7). The attractor also shows the ENSO dynamics, characterized by El Niño positive loops and normal La Niña conditions (neutral and negative values).
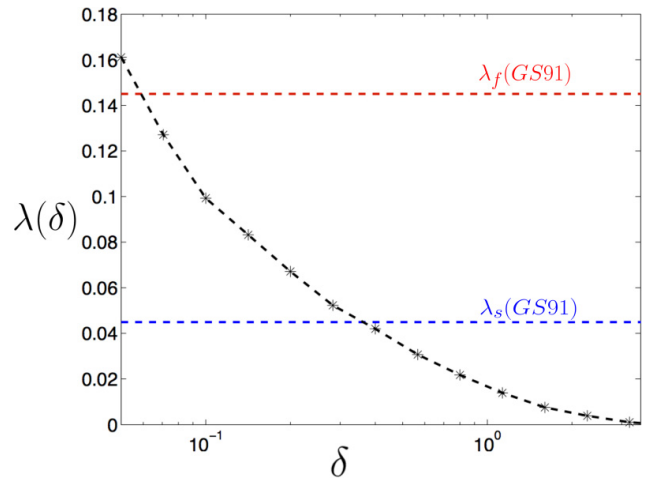
In the final step, the NINO3 time series of the CZ model were analyzed by the FSLE algorithm to infer its predictability. For the sake of brevity a detailed description of the computation of FSLE is not covered here. Interested readers are referred to the paper by Boffetta et al. (1998b).
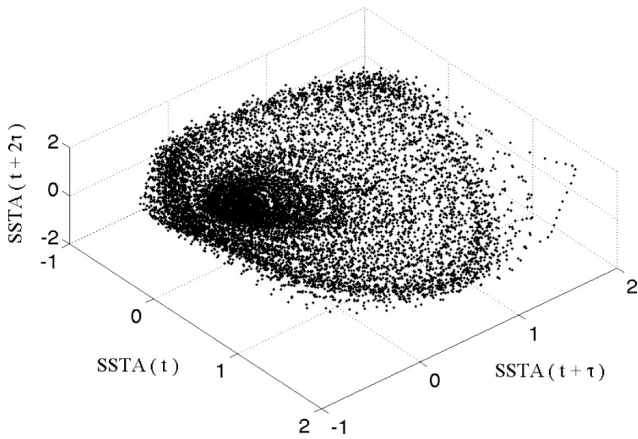
Fig. 7. Reconstructed phase space (three-dimensional projection) of SSTA of the NINO3 region from the CZ model.

Fig. 8. Scale-dependent Lyapunov exponents $\lambda(\delta)$ of the CZ model as a function of scale δ in the range [0.05, 1.5]. The dashed red line shows the Goswami and Shukla (1991) estimation for the fast mode growth rate λ_f and the dashed blue line the slow mode growth rate λ_s.

Figure 8 shows the plot of the FSLE $\lambda(\delta)$ as a function of the scale δ. The scales δ are defined on an embedded phase space with dimension $m = 9$, and a delay time $\tau_{corr} = 10$ months as suggested by the autocorrelation and mutual information. The metric used for delta is $\delta = \| \mathbf{x} - \mathbf{x}' \|$, see Fig. 1, and the choice for the initial size of δ_{min} is limited by the precision of a finite data set of N points that leads to a minimum length scale ϵ_0 below which the attractor structure cannot be resolved. The scales at which the correlation dimension curves, shown in Fig. 6, start to fluctuate tremendously due to the lack of neighbors indicate the minimum length scale. These scales are smaller than the average inter-point distance in the attractor in embedding space and δ_{min} can be approximated by $\epsilon_0 \approx L/N^{(1/d)}$, where L is the extent of the attractor and d is its correlation dimension (Farmer et al., 1983). In order to compute the FSLE, we performed a 50 000 yr-long run, which roughly gives a minimum length scale $\epsilon_0 \approx 0.05$ if we consider the attractor dimension of $d = 4$, which is in agreement with the behavior of the correlation dimension curves for scales $\epsilon < 0.04$ in Fig. 6. For values $\delta > 3$ the perturbation size is comparable to the variance of the NINO3 SSTA, rendering the FSLE meaningless (saturation value δ_{N_s}).

One noticeable feature in Figs. 8 and 9 is that they show very gradually changing curves for $\lambda(\delta)$ and T_p, which is rather different from the abrupt changes in the simple systems of Boffetta et al. (1998a) that have only two different timescales. As pointed out by Lorenz (1969), the errors in different scales in systems possessing many scales of motion tend to grow at different rates and saturate at different levels. First, let us consider very small amplitude perturbations $\delta = 0.05$ associated with errors in the smallest fastest-evolving scales of motion we can discern in this work. It is seen in Fig. 8 that for very small δ the magnitude of $\lambda(\delta = 0.05) \approx 0.16$ month^{-1} (doubling time of 4.3 months).
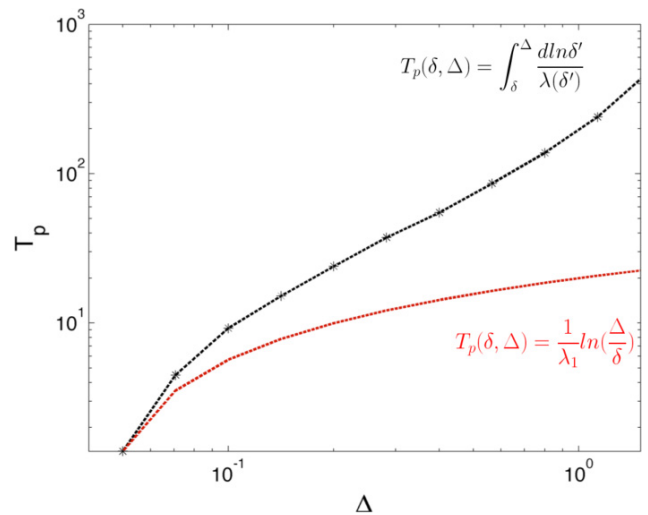
Fig. 9. Average error growing time T_p (months) of the CZ model as a function of the error tolerance level Δ based on: FSLE (black line) and the maximum Lyapunov exponent λ_{fast} (red line). Note that predictability inferred by assuming "infinitesimal" perturbations (dashed red line) is much smaller than that inferred by finite-size perturbations (black line).

Goswami and Shukla (1991), in a predictability study of the CZ model, found the fast growth rate to be $\lambda_f \approx 0.145$ month^{-1}, corresponding to a doubling time of 4.8 months. This matches the growth rate found here and we must underline that, like us, they do not consider the dependence of predictability on season or regime. Blumenthal (1991), following a predictability study involving principal oscillation patterns (POPs) but using the same model, found that there is a seasonality to error growth in the

CZ model, with spring starts showing the largest error growth. Blumenthal (1991) found that the doubling time for February and May starts is 4.2 months, while integrations starting in August and November show much less error growth with doubling times of 7 months and 9.5 months, respectively. Later on, Goswami et al. (1997) used a decomposition of model fields in terms of the model's EOFs, allowing them to introduce errors with a given spatial structure and to study growth of errors in all scales. Using a similar approach to Goswami and Shukla (1991) to compute error growth, but examining the seasonal and scale dependence, they found that growth of small or moderate error in the initial condition is always slow in winter forecasts and fast in forecasts started from spring of certain years. Furthermore, they concluded that the slow growth rate of errors (doubling time of about 15 months) is intrinsic to the model, whereas the fast growth rate (doubling time of about 5 months) comes from the coupling with the atmospheric winds and its interaction with the tropical wave dynamics.

The fast growth rate seems therefore to be closely related to the growth-phase predictability barrier also known as the "spring predictability barrier" (Moore and Kleeman, 1996; Chen et al., 2004; Yu et al., 2009). The spring predictability barrier has been explained in terms of the seasonal dependence of the air-sea coupling process, due to the seasonal movement of the Intertropical Convergence Zone, which is closest to the Equator, and SST in the east is warmest. The spring is also, of course, the period when the El Niño growth phase tends to occur, since the coupling between model atmosphere and ocean is such that small perturbations in the initial state are easily amplified. Samelson and Tziperman (2001) suggest that there is a predictability barrier associated with the growth phase of El Niño conditions instead of a spring barrier. That is, ENSO's predictability is smallest during the growth phase of El Niño conditions in the equatorial eastern Pacific, indicating that the growth mechanism of the disturbance is likely to be similar to that of the mechanism due to which the mature El Niño develops.

The mechanism that leads to a mature El Niño lies in the coupling with the atmospheric winds and its interaction with the tropical wave dynamics leading to the growth of coupled instabilities. In the CZ model, the model run is initiated with an imposed westerly wind anomaly that is held fixed for a given period and then removed. The westerly wind anomaly produces an initial thermocline depression that leads to an ocean heating anomaly, atmospheric convergence, latent heat release, then further downwelling and deepening of the thermocline (positive coupled feedback). The disequilibrium is carried by the ocean wave dynamics as eastward propagating equatorial Kelvin waves and westward propagating off-equatorial Rossby waves. In the central and eastern Pacific the Kelvin waves grow unstable if they have large wavelengths and are slow enough to stay within the coupling region so that the coupling process feeds back on the perturbation. The CZ model then shows the recurrence of warm events, deriving solely from self-interactions of the coupled system since there is no external forcing.

The CZ model was designed specifically to capture interannual variability of the large spatial scales of motion in the ocean. Therefore, the slow growth rate of errors is intrinsic to the ocean dynamics (slow model). On larger scales the growth rate is much slower and is associated with equatorial trapped Rossby wave timescales (ENSO mode). The perturbations of the thermocline also produce negative off-equatorial depth anomalies (that is, a shallowing signal of the thermocline) in the central Pacific that excite westward propagating Rossby waves. These Rossby waves are reflected off the western boundary as large-scale equatorial Kelvin waves (long wave approximation) and eventually arrive at the eastern Pacific months later, shallow the thermocline there and cause cooling of the SST. It is worth noting that by making a long wave approximation, one is assuming that all the energy associated with reflected Rossby waves goes into the largest Kelvin modes. Therefore, reflection becomes too efficient as it happens in the CZ model and is also enhanced by the use of unrealistic solid boundaries in this model. That means that the detection of the slow growth rate may be harder when considering more realistic models like CGCMs or in the observations.

Although a lot of attention has been given to the fast growth rate, the existence of slow growth in the coupled system as shown by Goswami and Shukla (1991) and Goswami et al. (1997) has been the basis for optimism for ENSO prediction at longer lead times. The slow growth rate found by Goswami and Shukla (1991) is $\lambda_s = 0.045\,\mathrm{month}^{-1}$, corresponding to a doubling time of 15.3 months. The slow timescale proposed by Goswami and Shukla (1991) actually comes from fitting their error curves, based on 151 initial conditions and 180 months long runs, with a linear combination of two processes having two timescales of error growth. Here we cannot point out a specific value for the slow growth rate, but a spectra of slow growth rates for the large scales. An equivalent slow growth rate to the one found by Goswami and Shukla (1991) corresponds to perturbation scales of $\delta \approx 0.4\,°\mathrm{C}$ as shown in Fig. 8. To put these growth rates into perspective, an initial error of 0.4 °C in SST would take about 7 months to grow to 1.5 °C (approximately the standard deviation of NINO3 SST anomalies) at the fast rate, and about 2 yr at the slow rate.

Another fact that can affect the estimation of growth rates is that, in the presence of regimes like in the CZ model (Fig. 4), the error growth rate given by the FSLE can be a highly fluctuating function of initial state. In particular, troughs in the large scales of FSLE spectra are shown to be a signature of slow regimes (in the slow system – ocean), whereas regimes occurring in the fast system (atmosphere) are shown to cause large peaks in the FSLE spectra where error growth rates far exceed those estimated from the maximal Lyapunov exponent (Mitchell and Gottwald, 2012).

Figure 9 shows the average error growing time T_p (in months) as a function of the error tolerance level Δ for a small uncertainty of fixed size $\delta = 0.05\,°C$ to grow to a value $\Delta = 1.5\,°C$, and is obtained by Eq. (6). If one considers a constant $\lambda(\delta)$, the integral reduces to Eq. (2). The black line in Fig. 9 corresponding to T_p is based on the FSLE results shown in Fig. 8. The red line in Fig. 9 represents the estimation of T_p given by Eq. (2) for a hypothetical system with a single (fast mode) Lyapunov exponent $\lambda_{fast} = 0.16\,month^{-1}$ in red. Observe that the predictability inferred by assuming infinitesimal perturbations (red line) and fast growth rate is much smaller than that inferred by finite-size perturbations (black line), illustrating the fact that large errors evolve in general with large-scale characteristic time, which thus rules large-scale predictability.

In the past, Goswami and Shukla (1991) and Blumenthal (1991) performed predictability studies of the CZ model using different methods from the FSLE. Goswami and Shukla (1991) found that the error growth has two timescales, the shorter timescale having a doubling time of approximately 4.8 months, while Blumenthal (1991) found a doubling time of 4.2 months for the spring season. The slow mode doubling time found by Goswami and Shukla (1991) is 15 months and is somewhat closer to the doubling time of 10 months found by Blumenthal (1991) for the winter season. Here we found, using the FSLE, a similar doubling time for the fast mode ($\sim$4.3 months). These earlier estimates of the growth rates are not very different from the fast growth rates found here. Although we cannot establish a specific doubling time for the slow mode (we have a spectra of slow growth rates for large scales), we believe that the ultimate limit on predictability in the CZ model is governed by the slow growth rates of errors intrinsic to the ENSO mode.

Although the FSLE is a relatively simple and very useful method for estimating the model predictability, it does not offer ways to infer the source of the fast and slow timescales in terms of spatial patterns of these finite-size perturbations that represent the directions of growing errors. However, it may provide tools to study the predictability of the real coupled ocean–atmosphere in the tropical Pacific, since it does not rely on the realization of twin experiments in order to compute the error growth like in the previous studies.

5 Conclusions

In this study we could identify different intrinsic timescales in the Cane–Zebiak intermediate model of the coupled ocean–atmosphere system of the tropical Pacific, with the shorter timescale showing a doubling time of approximately 5 months. The results also confirm that for systems with different intrinsic timescales, the slow varying quantities (i.e., large-scale features) have a longer predictability than the fast-evolving ones. Present-day CGCMs have useful ENSO prediction skill at lead times of $\sim$6 months, but the skill also depends strongly on season, ENSO phase, and ENSO intensity as shown in Jin et al. (2008). It seems that the skill of current models is limited by rapid growth of error, at a rate comparable to the fast rate identified in here and in the previous work on the predictability of the tropical Pacific coupled system.

Futhermore, assuming that the ENSO in a state-of-the-art CGCM is governed by chaotic nonlinear dynamics, we expect that the high-frequency noise or regime changes from the atmospheric internal dynamics can strongly influence the estimation of the λ_{fast} using the FSLE approach. However, we do not expect the predictability of the slow ENSO mode (λ_{slow}) to be significantly affected by the relatively high-frequency noise from the atmosphere, since the slow growth rate of errors is intrinsic to the ocean dynamics. Of course, we recognize that this assumption is the subject of considerable debate (e.g., Kirtman et al., 2005 for a discussion) and needs further investigation. The literature offers external stochastic forcing and chaos as two distinct possibilities for the irregularity of ENSO. This debate of stochastic forcing versus chaotic dynamics has important implications for understanding predictability, since the theoretical upper limit of predictability depends heavily on the mechanism for irregularity. Nevertheless, the approach may help diagnose the role of chaos in various CGCMs, and the applicability of this technique in higher complexity models like state-of-the-art CGCMs deserves further studies. We also expect that ENSO in most state-of-the-art CGCMs may also exhibit low-order dimensionality and that the essence of the method used here can be applied. The approach presented here in conjunction with the atmospheric noise reduction technique introduced by Kirtman and Shukla (2002) can be used to isolate the role of high-frequency atmospheric noise in the predictability of ENSO.

The FSLE is a relatively simple concept and very useful method for estimating the model predictability. However, it does not allow for the inference of the source of different timescales in terms of spatial patterns, nor does it provide answers to questions regarding the cascade of errors from one scale of motion to another. The main advantages of this technique relative to the others is that it is relatively simple to perform and allows the study of the predictability of the real coupled ocean–atmosphere in the tropical Pacific, since it does not rely on the realization of twin experiments in order to compute error growth as in the previous studies, only possible with coupled models.

Edited by: O. Talagrand
Reviewed by: G. Burgers and one anonymous referee

References

Albano, A. M., Muench, J., Schwartz, C., Mees, A. I., and Rapp, P. E.: Singular value decomposition and the Grassberger-Procaccia algorithm, Phys. Rev. A, 38, 3017–3026, 1988.

Aurell, E., Boffetta, G., Crisanti, A., Paladin, G., and Vulpiani, A.: Predictability in the large: An extension of the concept of Lyapunov exponent, J. Phys. A-Math. Gen., 30, 1–26, 1997.

Blumenthal, M. B.: Predictability of a coupled ocean–atmosphere model, J. Climate, 4, 766–784, 1991.

Boffetta, G., Crisanti, A., Paparella, F., Provenzale, A., and Vulpiani, A.: Slow and fast dynamics in coupled systems: A time series analysis view, Physica D, 116, 301–312, 1998a.

Boffetta, G., Giuliani, P., Paladin, G., and Vulpiani, A.: An extension of the Lyapunov analysis for the predictability problem, J. Atmos. Sci., 55, 3409–3412, 1998b.

Boffetta, G., Cencini, M., Falcioni, M., and Vulpiani, A.: Predictability: a way to characterize complexity, Phys. Rep., 356, 367–474, 2002.

Charney, J. G., Fleagle, R. G., Riehl, H., Lally, V. E., and Wark, D.: The feasibility of a global observation and analysis experiment, B. Am. Meteorol. Soc., 47, 200–220, 1966.

Chen, D., Cane, M. A., Kaplan, A., Zebiak, S. E., and Huang, D. J.: Predictability of El Niño over the past 148 years, Nature, 428, 733–736, 2004.

Farmer, J. D., Ott, E., and Yorke, J. A.: The dimension of chaotic attractors, Physica D, 7, 153–180, 1983.

Fraser, A. M. and Swinney, H. L.: Independent coordinates for strange attractors from mutual information, Phys. Rev. A, 33, 1134–1140, doi:10.1103/PhysRevA.33.1134, 1986.

Goswami, B. N. and Shukla, J.: Predictability of a coupled ocean atmosphere model, J. Climate, 3, 2–22, 1991.

Goswami, B. N. and Shukla, J.: Aperiodic variability in the Cane–Zebiak model: A diagnostic study, J. Climate, 5, 628–638, 1993.

Goswami, B. N., Rajendran, K., and Sengupta, D.: Source of Seasonality and Scale Dependence of Predictability in a Coupled Ocean-Atmosphere Model, Mon. Weather Rev., 125, 846–858, 1997.

Grassberger, P. and Procaccia, I.: Characterization of strange attractors, Phys. Rev. Lett., 50, 346–349, 1983.

Jin, E. K., Kinter, J. L., Wang, B., Park, C.-K., Kang, I.-S., Kirtman, B. P., Kug, J.-S., Kumar, A., Luo, J.-J., Schemm, J., Shukla, J., and Yamagata, T.: Current status of ENSO prediction skill in coupled ocean atmosphere models, Clim. Dynam., 31, 647–664, doi:10.1007/s00382-008-0397-3, 2008.

Kantz, H.: A robust method to estimate the maximal Lyapunov exponent of a time series, Phys. Lett. A, 185, 77–87, 1994.

Kantz, H. and Schreiber, T.: Nonlinear Time Series Analysis, 2nd edn., Cambridge University Press, Cambridge, UK, 2004.

Kirtman, B. P. and Min, D.: Multimodel Ensemble ENSO Prediction with CCSM and CFS, Mon. Weather Rev., 1372, 2908–2930, 2009.

Kirtman, B. P. and Shukla, J.: Interactive coupled ensemble: A new coupling strategy for GCMs, Geophys. Res. Lett., 29, 1029–1032, 2002.

Kirtman, B. P., Pegion, K., and Kinter, S. M.: Internal atmospheric dynamics and tropical Indo-Pacific climate variability, J. Atmos. Sci., 62, 2220–2233, 2005.

Lorenz, E. N.: Deterministic Nonperiodic Flow, J. Atmos. Sci., 20, 130–141, 1963.

Lorenz, E. N.: A study of the predictability of a 28-variable atmospheric model, Tellus, 17, 321–33, 1965.

Lorenz, E. N.: The predictability of a flow which possesses many scales of motion, Tellus, 21, 289–307, 1969.

Mitchell, L. and Gottwald, G. A.: On finite-size Lyapunov exponents in multiscale systems, Chaos, 22, 1–10, 2012.

Moore, A. M. and Kleeman, R.: The dynamics of error growth and predictability in a coupled model of ENSO, Q. J. Roy. Meteor. Soc., 122, 1405–1446, 1996.

Peña, M. and Kalnay, E.: Separating fast and slow modes in coupled chaotic systems, Nonlin. Processes Geophys., 11, 319–327, doi:10.5194/npg-11-319-2004, 2004.

Rosenstein, M. T., Collins, J. J., and De Luca, C. J.: A practical method for calculating largest Lyapunov exponents from small data sets, Physica D, 65, 117–134, 1993.

Samelson, R. M. and Tziperman, E.: Instability of the Chaotic ENSO: The Growth-Phase Predictability Barrier, J. Atmos. Sci., 58, 3613–3625, 2001.

Sauer, T., Yorke, J. A., and Casdagli, M.: Embedeology, J. Stat. Phys., 65, 579–616, 1991.

Shukla, J.: Predictability, in: Issues in atmospheric and oceanic modeling, Part II. Weather Dynamics, Academic Press, Inc., 28B 87–122, 1985.

Smagorinsky, J.: Problems and promises of deterministic extended range forecasting, B. Am. Meteorol. Soc., 50, 286–311, 1969.

Takens, F.: Detecting strange attractors in turbulences, in: Dynamical Systems and Turbulence, Springer-Verlag, Berlin, 898, 366–381, 1981.

Toth, Z. and Kalnay, E.: Ensemble forecasting at NMC: The generation of perturbations, B. Am. Meteorol. Soc., 74, 2317–233, 1993.

Toth, Z. and Kalnay, E.: Ensemble forecasting at NCEP and the breeding method, Mon. Weather Rev., 125(12), 3297–3319, 1997.

Tsonis, A. A.: Chaos: from theory to applications, Plenum, NY, 1992.

Tziperman, E., Stone, L., Cane, M. A., and Jarosh, H.: El-Niño chaos: overlapping of resonances between the seasonal cycle and the Pacific ocean–atmosphere oscillator, Science, 264, 72–74, 1994.

Vikhliaev, Y., Kirtman, B., and Schopf, P.: Decadal North Pacific Bred Vectors in a Coupled GCM, J. Climate, 20, 5744–5764, 2007.

Yu, Y. S., Duan, W. S., and Xu, H.: Dynamics of nonlinear error growth and season-dependent predictability of El Niño events in the Zebiak-Cane model, Q. J. Roy. Meteor. Soc., 135, 2146–2160, 2009.

Zebiak, S. E. and Cane, M. A.: A model El Niño/Southern Oscillation, Mon. Weather Rev., 115, 2262–2278, 1987.